An Optimization Approach for Hourly Ozone Simulation: A Case Study in Chongqing, China

Songyan Zhu , Qiaolin Zeng, Hao Zhu, Jian Xu , *Member, IEEE*,
Jianbin Gu, Yongqian Wang, and Liangfu Chen

Abstract— Continuous spatial knowledge is required to control the regional ozone pollution. Measurements from ground-level sites are beneficial to this goal, but their number is limited due to the huge expenses of site establishment, operation, and maintenance. Remote sensing seems a promising data source, but its application is challenged by bad weather conditions. Always covered by thick clouds, Chongqing, a populated industrial city in west China, is facing serious ozone pollution, but relevant studies here are relatively insufficient. Another alternative is estimating ozone by models. Well-performed models degrade in Chongqing partially due to the very complex terrain. Modeled hourly ozone does not agree with ground-level measurements. Therefore, an optimization approach is proposed to improve model estimates for such regions. This approach integrates the ground-level information (e.g., measured ozone and meteorology) through the employment of ResNet (Residual Network). ResNet overcomes the notorious vanishing gradient issue in classic neural networks, and the ability of learning complex systems is largely boosted. Ozone distribution is like a gray image that varies every second, which is not the case usually learned by ResNet. A color-image alike data structure is raised to address this "nonstill image" problem; according to the Taylor Expansion, polynomials can describe a complex system, and the errors are acceptable. To facilitate the usage in business operations, this approach is designed to be robust, inexpensive, and easy to use. The scheme of control site selection is discussed in detail. In cross-validations, this approach performs well, averaged R^2 is higher than 0.9 and the error is less than 5 μg/m^3.

I. INTRODUCTION

INCREASING levels of surface ozone have been threatening the globe since the 1970s. The precursor of tropospheric ozone, NO_2, mainly comes from vehicle and industry emissions. China has undergone rapid urbanization, hence its ozone pollution has become a region problem [1], [2]. In recent years, less-developed mountainous west China is speedily catching up its coastal east counterpart in various aspects, but surface ozone studies about the west cities are still insufficient.

Chongqing, situated in southwest China, is a populated industrialized municipality, and it is confronted with severe ozone-related issues. As a mountain city, its extremely undulating terrain influences the dispersion of ozone. About one-third days per year are foggy; Chongqing is also known as the "Fog City," and it is always covered by thick clouds [3]. The harsh weather conditions furthermore complicate the studies in Chongqing.

Continuous fine-resolution records are important to reduce ozone pollution, but the mainstream data sources show obvious defects in Chongqing. Ground-level sites provide accurate measurements, but it is impractical to deploy many long-term stable operation sites to cover a large region. In terms of coverage, satellite remote sensing provides low-cost ozone observation on a large scale. It seems promising, but the application of remote sensing in Chongqing is greatly restricted by the bad weather. By computer simulation, the chemical transport models (CTMs) can offer regional hourly ozone concentrations. The modeled ozone is estimated from emissions sources (e.g., inventories), meteorological fields, photochemical equations, and so on.

Representatives of the CTMs include Goddard Earth Observing System—Chemistry (GEOS-Chem), Model for OZone and Related chemical Tracers (MOZART), and Community Multiscale Air Quality Modeling System (CMAQ) [4]–[6]. Overall, these models have been globally validated in key regions, whereas the localized CMAQ is also widely adopted in China. In addition, models originated from China, like the nested air quality prediction modeling system (NAQ-PMS), exhibit high precision in middle and eastern China [7].
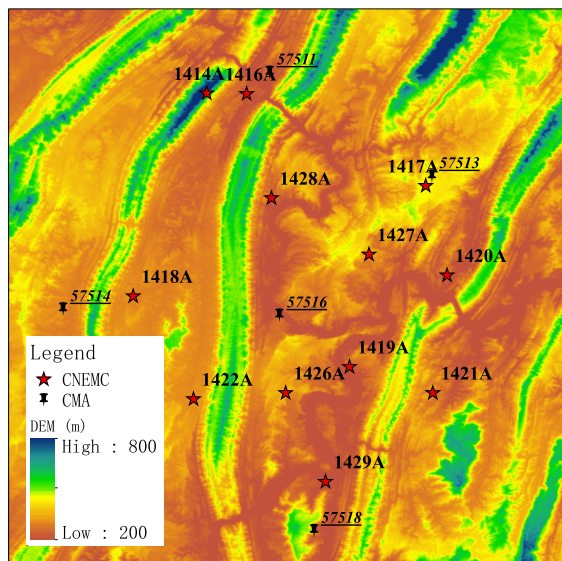
Fig. 1. Locations of the CNEMC (red stars) for ozone measurements and CMA (black pushpins) meteorology sites. The base-map depicts Chongqing's terrain. Only ozone data available CNEMC sites are used.
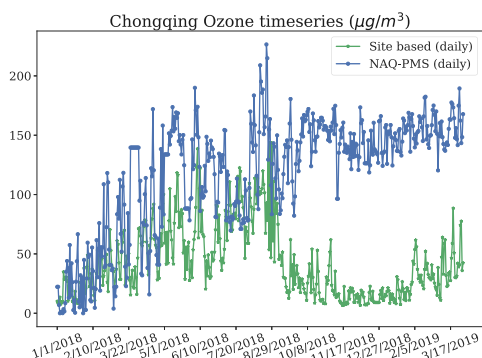

Fig. 2. Averaged daily O_3 timeseries in Chongqing in the time range used in this study. The discrepancy between ground measurements (green) and NAQ-PMS (blue) at 500 m is very large. Unit of modeled ozone is converted to $\mu g/m^3$.

Fig. 3. Flowchart of the approach from data collection to application. The core steps include data preparation, unification, network training, and validation.

The reality is not very optimistic. Despite many advantages, models face great challenges in Chongqing. First, it is harder to quantify the atmospheric processes of ozone here. Also, defining the "surface" is difficult in models, due to Chongqing's extremely uneven terrain. Fig. 1 demonstrates the terrain of urban Chongqing and locations of ground-level sites. The altitude here varies from lower 200 m to higher than 800, whereas the layers' altitudes in NAQ-PMS are fixed. Fig. 2 shows the comparison between Chongqing's daily NAQ-PMS ozone simulations and site-based measurements. The modeled ozone shown in the figure is at 500 m, which is the lowest layer in NAQ-PMS. The correlation coefficient between simulations and measurements is lower than 0.5. Apparently, the performance of the model in Chongqing is not very satisfactory, although NAQ-PMS is one of the most excellent models for China.

To optimize the modeled ozone, this work proposes an approach by introducing measured ground-level information

learned by a neural network. The problem here is that neural networks usually recognize the still objects in satellite images, but ozone distribution varies constantly [8]–[13]. The ResNets (Residual Networks) overcome the vanishing gradient problem in classic deep neural networks, so that they can process more complex tasks [15]. Besides, a new data structure is also created to help address this problem.

II. APPROACH FRAMEWORK

Fig. 3 gives the workflow for the proposed approach (referred to as the approach hereafter). The framework of the approach comprises of four major parts: 1) data unification including spatial interpolation and resampling; 2) control site selection; 3) 3-D structural data set construction; and 4) neural network training and evaluation.

A. Data Unification

The study area is urban Chongqing where enough sites for validation exist. NAQ-PMS has 12 altitude layers, and the lowest one (500 m) is used. This area contains 12 China National Environmental Monitoring Centre (CNEMC) sites providing hourly ground-level ozone measurements, which can be used as control sites or validation sites. There are

four China Meteorological Administration (CMA) sites offering hourly measured meteorological parameters. Here, the used parameters are instantaneous wind speed, wind direction, precipitation per hour, temperature, relative humidity, pressure, and visibility. All data used are from January 1, 2018, to April 10, 2019, covering more than one year, because ozone shows explicit seasonal patterns [14].

Preprocessing before feeding data to the neural network includes data cleaning, resampling, and interpolation. Original meteorology records have many invalid readings, and all these readings are removed or replaced. A bilinear resampling is carried out because the spatial resolutions of different NAQ-PMS versions are not consistent ($\sim$0.15° and $\sim$0.25°). NAQ-PMS and CMA data at the geolocations of CNEMC sites are obtained by interpolation, thereby 12 data groups are generated. Each group is a time series of hourly records. Each hourly record comprises meteorological parameters, modeled and measured ozone at that time.

B. Control Points Selection

The concept of the control site is inspired by the satellite image geometric correction. Briefly speaking, the control sites are CNEMC sites used to improve the modeled ozone. Other sites are called as validation sites. The number and position of control sites are crucial to the balance of the approach's performance and practicality.

In terms of performance, too few control sites will result in low accuracy. Values outside the envelope of control sites are derived from extrapolation, which is less controllable and reliable than interpolation. For the ozone regulation departments, too many control sites will increase the burden of the practical running. In this study, four sites are used as control sites. Control sites are not supposed to be too close or too far from each other. In addition, ozone concentration is related to terrain, and site elevation should be considered in the selection as well.

In the experiment, the optimal selection marked as "scenario 1" and other three typical selections (scenarios 2 to 4) are given. Due to the experiment sufficiency concerns, ten more supplementary experiments are also carried out. Scenario 1 uses four control sites to cover a large region as possible. Site 1414A is hundreds of meters higher than other sites, and it is treated as a control site in scenario 1. In scenario 2, site 1414A is replaced by a lower nearby site to assess the impact of elevation. Sites in the area center are selected as control sites in scenario 3 to test whether the approach is very biased by extrapolation. Regarding the influence of distance, sites located on the south edge are selected as control sites in scenario 4. Southern sites are the farthest from 1414A, thus results can be compared with scenarios 2 and 3. Failure modes are examined in the supplementary experiments by changing the selection of control sites more strictly.

C. Data Structure Design and Modeling

ResNet is a compelling groundbreaker in deep neural networks. Classic back-propagation networks can represent nonlinear functions, but their simple architectures suffer from
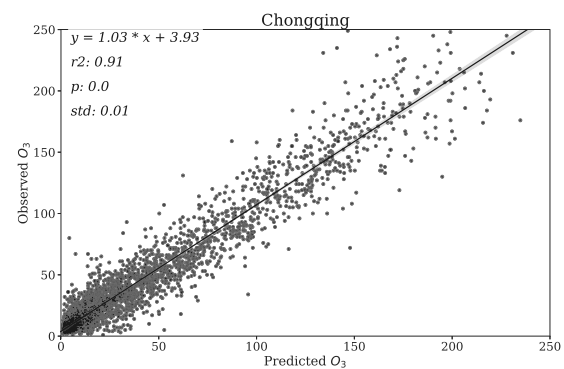

Fig. 4. Results of the approach validation at the scale of the whole study region in the optimal scenario (i.e., scenario 1). Scatter plot of ResNet prediction (X-axis) and ground CNEMC measured ozone (Y-axis) from the test sets is presented. Linear regression, R^2, p value, and standard deviation are given as well. Measured ozone in the test sets are not involved in ResNet training at all, which is used for validation only.

the overfitting problem. Deeper architecture can address this problem, but attempts by stacking layers failed due to the notorious vanishing gradient problem. In deep networks, the gradient approaches infinitely small (i.e., vanishing) by repeated multiplication in back-propagation. The philosophy of ResNet is "discarding" some information [15]. In terms of implementation, stacked layers fit a residual mapping, with the support of "identity shortcut connection" which skips some layers. ResNet features a greatly enhanced performance in image recognition, therefore an 18-layer ResNet (ResNet-18) is employed here. It is possible to train up to hundreds of layers with ResNet but the trade-off is huge time-consumption and much better hardware. It is not very friendly to departments with limited budgets, and ResNet-18 shows satisfactory capability.

A "fake colorful image" alike data structure is proposed to take ResNet's advantage of learning structural and spectral information. As argued in literature, a complicated system (e.g., atmosphere) can be approximated by polynomials through the Taylor Expansion, and the uncertainty is a high-order infinitesimal [16]. Accordingly, a three-order Taylor Expansion is applied to every record of validation sites at each timestamp. The coordinates of sites are known, and a record of the validation site consists of four control sites' information (network inputs) and measured ozone at this validation site (ground-truth). As usual, data sets are randomly split into train-sets and test-sets, and test-sets are not involved in network training at all.

III. RESULTS AND DISCUSSION

A. Approach Results for Four Scenarios

Fig. 4 exhibits the comparison between the approach's results and measured ground-level ozone. The comparison given is in scenario 1, and all validation sites are involved in the evaluation. Apparently, the accuracy of NAQ-PMS ozone at 500 m is significantly improved. The R^2 score of test-sets in Chongqing increases from less than 0.5 to $\sim$0.91 (p value $\ll$ 0.05).

TABLE I

STATISTICAL METRICS OF THE APPROACH VALIDATION IN
SCENARIOS 1 AND 2. CONTROL SITES ARE REPRESENTED
BY HYPHENS. PCC: PEARSON CORRELATION COEFFICIENT;
STD.: STANDARD DEVIATION

Code	Scenario 1			Scenario 2		
	PCC	R^2	Std.	PCC	R^2	Std.
1414A	-	-	-	0.86	0.74	0.03
1416A	0.97	0.94	0.01	-	-	-
1417A	-	-	-	-	-	-
1418A	-	-	-	-	-	-
1419A	0.95	0.89	0.02	0.96	0.91	0.02
1420A	0.95	0.90	0.02	0.95	0.90	0.02
1421A	0.96	0.92	0.01	0.97	0.94	0.01
1422A	0.97	0.94	0.01	0.96	0.93	0.01
1426A	0.97	0.93	0.01	0.97	0.94	0.01
1427A	0.96	0.92	0.01	0.95	0.91	0.02
1428A	0.96	0.92	0.01	0.98	0.96	0.01
1429A	-	-	-	-	-	-
Whole	0.96	0.91	0.01	0.95	0.91	0.01

TABLE II

STATISTICAL METRICS OF THE APPROACH VALIDATION IN
SCENARIOS 3 AND 4, SEE TABLE I

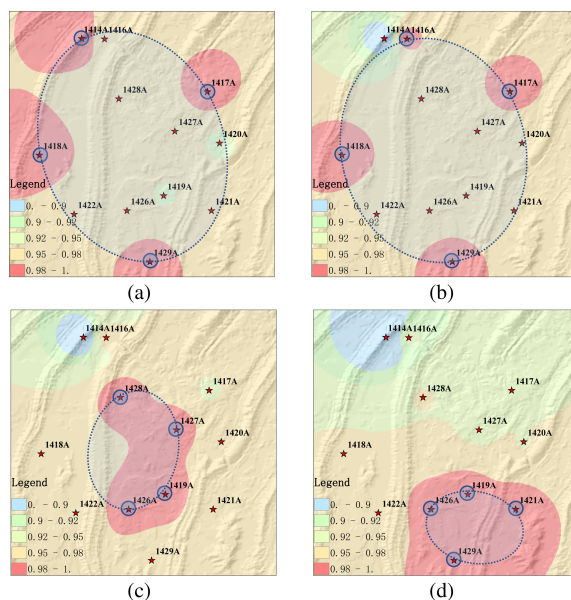| Code	Scenario 3			Scenario 4		
	PCC	R^2	Std.	PCC	R^2	Std.
1414A	0.85	0.73	0.03	0.83	0.68	0.03
1416A	0.97	0.94	0.01	0.94	0.88	0.02
1417A	0.95	0.89	0.02	0.94	0.88	0.02
1418A	0.96	0.93	0.01	0.96	0.91	0.01
1419A	-	-	-	-	-	-
1420A	0.96	0.92	0.02	0.95	0.90	0.02
1421A	0.96	0.92	0.01	-	-	-
1422A	0.95	0.90	0.02	0.96	0.92	0.01
1426A	-	-	-	-	-	-
1427A	-	-	-	0.94	0.89	0.02
1428A	-	-	-	0.95	0.91	0.02
1429A	0.96	0.92	0.01	-	-	-
Whole	0.96	0.91	0.01	0.96	0.92	0.01

Fig. 5. Regional correlation coefficient distribution of the four scenarios between measured ozone and ResNet-18 predictions. (a)–(d) Scenarios 1–4, respectively. Similar to Fig. 4, the predictions are results from the approach, and data used to demonstrate here are from the test sets only. Below the correlation distribution is the terrain map. The red stars are the CNEMC sites, circled ones among them are the control sites, and others are the validation sites.

Evaluations details for all four scenarios are summarized in Tables I and II. In addition, Fig. 5 gives a more intuitive demonstration of how well does the approach performs. It shows the correlation between approach results and ground-level measurements. Indices to assess the approach are the Pearson correlation coefficient (PCC) with p values, R^2 score, and standard deviation (std). Overall, p values and standard deviations are small enough for all sites in all scenarios, e.g., p values are all far less than 0.05. In scenario 1, the approach shows excellent performance at every validation site. For almost all validation sites, the R^2 scores are higher than 0.9 except at site 1419A. The high correlations indicate that the approach is feasible in Chongqing.

Scenario 2 is a comparative experiment to explore the impact attributed by elevation. Only one control site is replaced compared to scenario 1. Except site 1414A, there is no obvious discrepancy in the metrics between scenarios 1 and 2. Interestingly, sites 1414A and 1416A are horizontally close compared to all other sites, whereas the result at 1414A is the worst. Evaluation metrics at other farther validation sites are much better. The huge elevation difference may be prominent in affecting the approach performance.

It is still uncertain if the issue raised in scenario 2 is caused by terrain, because in both scenarios, one of sites 1414A and 1416A is used as a control site. Accordingly, scenarios 3 and 4 are used to discuss this issue furthermore. In these cases, both 1414A and 1416A are used as validation sites; hence, a more reasonable deduction can be derived from a direct comparison. At the scale of the whole study area, PCC and R^2 metrics of scenarios 3 and 4 agree with each other and the two previous scenarios. The PCC is about 0.95 while the R^2 is about 0.91. As suggested in Table II, first, the approach tolerates extrapolation to some extent. All control sites in scenario 3 are situate in the center of the study area, and evaluation metrics are consistent with scenarios 1 and 2. Meanwhile, distance is influential. Target sites (i.e., 1414A and 1416A) lie in northern Chongqing, thus all the control sites are on the south edge. The approach degrades totally in the middle and northern parts, especially at the target sites. For example, the R^2 at 1416A decreases from 0.94 to 0.88. Apparently, it is the terrain that accounts for the less good results at site 1414A. Regarding all four scenarios, NAQ-PMS optimization results at 1414A degrade with increasing distances, but the variations are not large. Moreover, the results of site 1417A also agree with this assumption about elevation. Site 1417A is located in the mid-east of the study region. Its altitude (about 500 m) is higher than the average of other sites (about 200 m), although it's lower than 1414A (about 800 m). In scenario 3, despite the close distance to control sites, the R^2 of 1417A is a little lower than other validation sites. Reasonably, its metrics decrease a bit in scenario 4, and this agrees with our argument.

TABLE III

STATISTICAL METRICS FOR R^2 SCORES IN CROSS VALIDATION AT THE SITE LEVEL. THE APPROACH IS TESTED AT EACH VALIDATION SITE FOR EVERY EXTRA TESTING

Case	Min	Max	Mean	Std.
exc. (S) *	0.89	0.94	0.91	0.02
exc. (N)	0.73	0.94	0.89	0.07
exc. (W)	0.89	0.95	0.92	0.02
exc. (E)	0.89	0.94	0.91	0.02
pos. (NE) **	0.83	0.92	0.89	0.03
pos. (NW)	0.83	0.90	0.88	0.03
pos. (SW)	0.70	0.94	0.89	0.08
pos. (W)	0.85	0.93	0.89	0.03
pos. (E)	0.68	0.94	0.88	0.09
pos. (SE)	0.71	0.93	0.88	0.07

* Control site in south (S) is excluded (exc.) from the selection. Initials within parenthesises represent positions, e.g. N and NE stand for north and northeast, respectively.
** All the four control sites are located in position (pos.) northeast (NE).

B. Performance in Extra Cross Validations

More extreme cases are tested to assess the robustness of the proposed approach. First, four optimal control sites are excluded from testing, individually. Subsequently, control sites are geographically located in different directions. Contributions from validation sites' geographical locations and their properties are estimated in these cross-testings. Table III provides the statistical estimates among validation sites in these rigorous cross-testings. Correlation coefficients are all higher than the corresponding R^2 scores, and all p values are smaller than 0.05. Due to the limited letter length, only details of R^2 are given here. For all cases, the mean R^2 scores are about 0.9, and the standard deviations among sites are smaller than 0.1. Minimums lower than 0.8 are all observed at site 1414A. Results of the supplementary cross-testing infer that the approach is reliable in Chongqing, and the selection of control sites should take the site elevation into consideration.

IV. CONCLUSION

In this study, an optimization approach is proposed to improve the surface ozone modeling for complex terrain. Chongqing, facing ozone threats and always covered by clouds, is an ideal place example to carry out the approach.

One key suggestion of this work is to simplify the continuously varying ozone and meteorology as "still images" by Taylor Expansion. Three-order polynomials are used to express the ozone distribution, and their uncertainties are higher order infinitesimals. Attributed to the proposed data structure, the uncertainties of the approach are less than 5 μg/m^3. Overall, the R^2 scores are about 0.9 and the correlation coefficients are higher.

Indicated by cross-testings, this approach is robust in Chongqing, and its application in other similar regions can be very encouraging. It tolerates extrapolation to some extent, and the distance between control sites can be as large as 50 km. Its simple architecture, affordable economical costs, and low requirements on fancy hardware make this approach feasible in business operations.

It is noteworthy that there is also a limitation in this approach. The averaged elevation difference between control sites and validation sites should be less than 800 m, and less than 400 m would be better. In the future, elevation information will be considered in the network, because only 12 sites exist in Chongqing now.

REFERENCES

[1] K. Li, D. J. Jacob, H. Liao, L. Shen, Q. Zhang, and K. H. Bates, "Anthropogenic drivers of 2013–2017 trends in summer surface ozone in China," *Proc. Nat. Acad. Sci. USA*, vol. 116, no. 2, pp. 422–427, Jan. 2019.

[2] X. Huang, J. Zhao, J. Cao, and Y. Song, "Spatial-temporal variation of ozone concentration and its driving factors in China," *Huan Jing Ke Xue=Huanjing Kexue*, vol. 40, no. 3, pp. 1120–1131, 2019.

[3] D. Liu, Z. Li, W. Yan, and Y. Li, "Advances in fog microphysics research in China," *Asia–Pacific J. Atmos. Sci.*, vol. 53, no. 1, pp. 131–148, Feb. 2017.

[4] D. Byun and K. L. Schere, "Review of the governing equations, computational algorithms, and other components of the models-3 community multiscale air quality (CMAQ) modeling system," *Appl. Mech. Rev.*, vol. 59, no. 2, pp. 51–77, 2006.

[5] S. Pawson *et al.*, "Goddard Earth Observing System chemistry-climate model simulations of stratospheric ozone-temperature coupling between 1950 and 2005," *J. Geophys. Res.*, vol. 113, no. D12, 2008.

[6] L. K. Emmons *et al.*, "Description and evaluation of the model for ozone and related chemical tracers, version 4 (MOZART-4)," *Geosci. Model Dev.*, vol. 3, pp. 43–67, Jan. 2010.

[7] Z. Wang, T. Maeda, M. Hayashi, L.-F. Hsiao, and K.-Y. Liu, "A nested air quality prediction modeling system for urban and regional scales: Application for high-ozone episode in Taiwan," *Water, Air, Soil Pollut.*, vol. 130, nos. 1–4, pp. 391–396, Aug. 2001.

[8] Y. Sun, Q. Zeng, B. Geng, X. Lin, B. Sude, and L. Chen, "Deep learning architecture for estimating hourly ground-level PM2.5 using satellite remote sensing," *IEEE Geosci. Remote Sens. Lett.*, vol. 16, no. 9, pp. 1343–1347, Sep. 2019.

[9] D. J. Lary, A. H. Alavi, A. H. Gandomi, and A. L. Walker, "Machine learning in geosciences and remote sensing," *Geosci. Frontiers*, vol. 7, no. 1, pp. 3–10, 2016.

[10] M. Qin, F. Xie, W. Li, Z. Shi, and H. Zhang, "Dehazing for multispectral remote sensing images based on a convolutional neural network with the residual architecture," *IEEE J. Sel. Topics Appl. Earth Observ. Remote Sens.*, vol. 11, no. 5, pp. 1645–1655, May 2018.

[11] E. Maggiori, Y. Tarabalka, G. Charpiat, and P. Alliez, "Fully convolutional neural networks for remote sensing image classification," in *Proc. IEEE Int. Geosci. Remote Sens. Symp. (IGARSS)*, Jul. 2016, pp. 5071–5074.

[12] R. Alshehhi, P. R. Marpu, W. L. Woon, and M. D. Mura, "Simultaneous extraction of roads and buildings in remote sensing imagery with convolutional neural networks," *ISPRS J. Photogramm. Remote Sens.*, vol. 130, pp. 139–149, Aug. 2017.

[13] X. Xu, W. Li, Q. Ran, Q. Du, L. Gao, and B. Zhang, "Multisource remote sensing data classification based on convolutional neural network," *IEEE Trans. Geosci. Remote Sens.*, vol. 56, no. 2, pp. 937–949, Feb. 2018.

[14] R. Su *et al.*, "Exploration of the formation mechanism and source attribution of ambient ozone in Chongqing with an observation-based model," *Sci. China Earth Sci.*, vol. 61, no. 1, pp. 23–32, Jan. 2018.

[15] K. He, X. Zhang, S. Ren, and J. Sun, "Deep residual learning for image recognition," in *Proc. IEEE Conf. Comput. Vis. Pattern Recognit. (CVPR)*, Jun. 2016, pp. 770–778.

[16] M. Pourahmadi, "Taylor expansion of and some applications," *Amer. Math. Monthly*, vol. 91, no. 5, pp. 303–307, May 1984.